

Synthesis and Characterization of a Series of Bis(oxo/thiophosphinic)diamido Yttrium Complexes and Their Application as Initiators for Lactide Ring-Opening Polymerization

Rachel H. Platel, Linda M. Hodgson, Andrew J. P. White, and Charlotte K. Williams*

Department of Chemistry, Imperial College London, London, SW7 2AZ, U.K.

Received April 30, 2007

The syntheses, structures, and lactide polymerization initiation are reported for a series of novel $\{[N,N'-1,3\text{-bis}(P,P'\text{-di-isopropoxyphosphinic})\text{-}2,2\text{-dimethylpropylenediamido}\}\text{(amido)yttrium}\}$ complexes and contrasted with $\{[N,N'-1,3\text{-bis}(P,P'\text{-di-isopropylthiophosphinic})\text{-}2,2\text{-dimethylamido}\}\text{bis}(\text{trimethylsilyl})\text{-amido}\}$ yttrium]. The syntheses of the novel $\{[N,N'-1,3\text{-bis}(P,P'\text{-di-isopropoxyloxo/thiophosphinic})\text{-}2,2\text{-dimethylpropylenediamido}\}\text{(amido)yttrium}\}$ complexes were achieved in excellent yields by reaction of the $N,N'-1,3\text{-bis}(P,P'\text{-di-isopropoxyloxo/thiophosphinic})\text{-}2,2\text{-dimethylpropylenediamine}$ ligands with $[Y(\text{NR}_2)_3 \cdot x\text{THF}]$ ($R = \text{SiMe}_3, \text{SiMe}_2\text{H}, i\text{-Pr}, x = 0, 2$). The new complexes were characterized by NMR and IR spectroscopies, elemental analyses, and for $R = \text{SiMe}_2\text{H}$ X-ray crystallography. The solution and solid-state structures were compared using 2D NMR techniques and in particular using pulsed gradient spin echo spectroscopy (PGSE) to derive the solution hydrodynamic radius and compare it to that calculated from the X-ray crystal structure: the $\{[N,N'\text{-bis}(P,P'\text{-di-isopropoxyphosphinic})\text{-}2,2\text{-dimethylpropylenediamido}\}\text{(amido)yttrium}\}$ complexes were all dimeric in both the solid state and solution. They showed unusual structures where each ligand has one oxophosphinic group bonded to a single yttrium center and one oxophosphinic group bonded to two yttrium centers. The new complexes were tested as lactide polymerization initiators; they all showed very high activities. The degree of polymerization control exerted by the novel initiators was related to the size of the initiating amide group and the structure of the complex.

Introduction

Lactide polymerization is attracting attention as a viable method to produce degradable plastics from renewable resources.¹ Polylactide is manufactured in the U.S. and on a smaller scale in both the E.U. and Japan; it is used in packaging, fibers and in medicine as a degradable matrix or as a vector in drug delivery.^{2,3} The life cycle of polylactide can be carbon neutral because the monomer, lactide, is produced by the fermentation of corn or sugar beet. The ring-opening polymerization (ROP) of lactide, initiated by metal complexes, is a useful route, as it yields polymers with tunable molecular weights and exerts tight control over the polymers' physical and chemical properties.^{4,5} The ROP is now widely accepted to occur via a coordination–insertion mechanism, and it has been experimentally verified by end group analysis and recently by calculations.^{4–6} However, the rate-determining steps and key transition states/intermediates are still ambiguous. While a range of different metals will initiate the polymerization, those that will do so with viable control and activity are still limited to Al(III), Sn(II), Ln(III), Mg(II), Ca(II), and Zn(II) complexes.^{4,5}

Homoleptic metal alkoxides and amides are known to initiate the polymerization, but they are hampered by poor solubility, low activity, and a lack of polymerization control. The use of ancillary ligands to generate single-site metal complexes has shown superior activity and control. The choice of metal complex is thus a key factor in mediating the polymerization.

Y(III) initiators are among the most active of all lactide polymerization initiators. Indeed the fastest are the homoleptic yttrium alkoxides reported by Dupont.⁷ There are now several other examples of yttrium alkoxides and aryloxides, including some single-site complexes.^{8–13} Recently a number of groups have reported single-site yttrium and scandium amide initiators,^{14–22} including single-site initiators that show good stereocontrol.^{16,18,20} However, despite their excellent potential,

(1) Ragauskas, A. J.; Williams, C. K.; Davison, B. H.; Britovsek, G.; Cairney, J.; Eckert, C. A.; Fredrick, W. J., Jr.; Hallett, J. P.; Leak, D. J.; Liotta, C. L.; Mielenz, J. R.; Murphy, R.; Templer, R.; Tschaplinski, T. *Science* **2006**, *311*, 484.

(2) Amass, W.; Amass, A.; Tighe, B. *Polym. Int.* **1998**, *47*, 89.

(3) Drumright, R. E.; Gruber, P. R.; Henton, D. E. *Adv. Mater.* **2000**, *12*, 1841.

(4) O'Keefe, B. J.; Hillmyer, M. A.; Tolman, W. B. *Dalton Trans.* **2001**, 2215.

(5) Dechy-Cabaret, O.; Martin-Vaca, B.; Bourissou, D. *Chem. Rev.* **2004**, *104*, 6147.

(6) Marshall, E. L.; Gibson, V. C.; Rzepa, H. S. *J. Am. Chem. Soc.* **2005**, *127*, 6048.

(7) McLain, S. J.; Ford, T. M.; Drysdale, N. E. *Polym. Prepr.* **1992**, *33*, 463.

(8) Stevels, W. M.; Ankone, M. J. K.; Dijkstra, P. J.; Feijen, J. *Macromolecules* **1996**, *29*, 3332.

(9) Simic, V.; Spassky, N.; Hubert-Pfalzgraf, L. G. *Macromolecules* **1997**, *30*, 7338.

(10) Ovitt, T. M.; Coates, G. W. *J. Am. Chem. Soc.* **1999**, *121*, 4072.

(11) Chamberlain, B. M.; Sun, Y.; Hagadorn, J. R.; Hemmesch, E. W.; Young, V. G., Jr.; Pink, M.; Hillmyer, M. A.; Tolman, W. B. *Macromolecules* **1999**, *32*, 2400.

(12) Chamberlain, B. M.; Jazdzewski, B. A.; Pink, M.; Hillmyer, M. A.; Tolman, W. B. *Macromolecules* **2000**, *33*, 3970.

(13) Ovitt, T. M.; Coates, G. W. *J. Am. Chem. Soc.* **2002**, *124*, 1316.

(14) Aubrecht, K. B.; Chang, K.; Hillmyer, M. A.; Tolman, W. B. *J. Polym. Sci.: Polym. Chem.* **2001**, *39*, 284.

(15) Ma, H.; Spaniol, T. P.; Okuda, J. *Dalton Trans.* **2003**, 4770.

(16) Cai, C.-X.; Amgoune, A.; Lehmann, C. W.; Carpentier, J.-C. *Chem. Commun.* **2004**, 330.

(17) Ma, H.; Okuda, J. *Macromolecules* **2005**, *38*, 2665.

(18) Amgoune, A.; Thomas, C. M.; Roisnel, T.; Carpentier, J.-C. *Chem.-Eur. J.* **2006**, *12*, 169.

Y(III) initiators are not as well developed as other metals, due in part to their synthetic complexity. Furthermore, the most successful ligand systems explored to date are all phenoxide derivatives, such as salens, 1, ω -dithialkanediyl-bridged bis-(phenolates), and bis(phenoxy) amines.^{10,13,15–18,20,22} There is scope for the development of new ligand classes, in particular those that will confer distinct electronic and coordination environments.

We are investigating the preparation of well-defined heteroleptic yttrium amido complexes of the type [LY(NR₂)], where L is an ancillary ligand and NR₂ is a bulky amido group, as they have previously shown very good activity for lactide ring-opening polymerization.¹⁹ Thus to prepare the target initiators, ancillary ligands (L) are required that are multidentate with a formal dinegative charge and that are sufficiently sterically protected to prevent complex redistribution reactions. Furthermore, recent lactide polymerization results indicate that ancillary ligands with “soft” donors such as amide and thioether groups are promising alternatives to hard alkoxide or phenoxide donors, as they enable high activity while maintaining high degrees of polymerization control.^{15,17,19,20} The non-metallocene coordination chemistry of yttrium has been nicely reviewed recently by Piers et al., who point out that a major challenge is steric protection of the metal center.²³ A range of sterically hindered, dianionic N-coordinated yttrium complexes have been investigated, including diamides^{24–26} and tridentate diamides incorporating a neutral ether, amine, or pyridyl donor.^{26–28} Yttrium also supports larger coordination numbers, and so polydentate dianionic N-coordinating ligands such as bis(amidates),^{29,30} bis(amino)troponimines,³¹ bis(β -diketiminates),³² bis(sulfonamides),³³ bis(aminopyridines),³⁴ bis(iminophosphonamides),³⁵ macrocycles,^{36,37} and porphyrins³⁸ have also been reported. Recently, Livinghouse et al. reported that bis(thiophosphonic)-diamine ligands used *in situ* with [Y{N(SiMe₃)₂}₃] led to a series of highly active and enantioselective hydroamination catalysts.³⁹

(19) Hodgson, L. M.; White, A. J. P.; Williams, C. K. *J. Polym. Sci.: Polym. Chem.* **2006**, 6646.

(20) Ma, H.; Spaniol, T. P.; Okuda, J. *Angew. Chem., Int. Ed.* **2006**, 45, 7818.

(21) Alaaeddine, A.; Amgoune, A.; Thomas, C. M.; Dagorne, S.; Bellemin-Lapponnaz, S.; Carpentier, J.-F. *Eur. J. Inorg. Chem.* **2006**, 3652.

(22) Westmoreland, I.; Arnold, J. *Dalton Trans.* **2006**, 4155.

(23) Piers, W. E.; Emslie, D. J. H. *Coord. Chem. Rev.* **2002**, 233–234, 131.

(24) Goutchev, T. I.; Tilley, T. D. *Organometallics* **1999**, 18, 2896.

(25) Cloke, F. G. N.; Elvidge, B. R.; Hitchcock, P. B.; Lamarche, V. M. *E. J. Chem. Soc., Dalton Trans.* **2002**, 2413.

(26) Estler, F.; Eickerling, G.; Herdtweck, E.; Anwender, R. *Organometallics* **2003**, 22, 1212.

(27) Graf, D. D.; Davis, W. M.; Schrock, R. R. *Organometallics* **1998**, 17, 5820.

(28) Skinner, M. E. G.; Mountford, P. *J. Chem. Soc., Dalton Trans.* **2002**, 1694.

(29) Bambirra, S.; Meetsma, A.; Hessen, B.; Teuben, J. H. *Organometallics* **2001**, 20, 782.

(30) Hill, M. S.; Hitchcock, P. B.; Mansell, S. M. *Dalton Trans.* **2006**, 1544.

(31) Roesky, P. W. *Chem. Soc. Rev.* **2000**, 29, 335.

(32) Vitanova, D. V.; Hampel, F.; Hultsch, K. C. *Dalton Trans.* **2005**, 1565.

(33) Görlitzer, H. W.; Spiegler, M.; Anwender, R. *Eur. J. Inorg. Chem.* **1998**, 1009.

(34) Noss, H.; Oberthür, M.; Fischer, C.; Kretschmer, W. P.; Kempe, R. *Eur. J. Inorg. Chem.* **1999**, 2283.

(35) Ahmed, S.; Hill, M. S.; Hitchcock, P. B.; Mansell, S. M.; St. John, O. *Organometallics* **2007**, 26, 538.

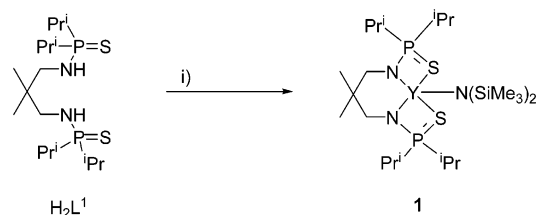
(36) Lee, L.; Berg, D. J.; Bushnell, G. W. *Inorg. Chem.* **1994**, 33, 5302.

(37) Fryzuk, M. D.; Love, J. B.; Rettig, S. J. *J. Am. Chem. Soc.* **1997**, 119, 9071.

(38) Schaverien, C. J.; Orpen, A. G. *Inorg. Chem.* **1991**, 30, 4968.

(39) Kim, Y. K.; Livinghouse, T.; Horino, Y. *J. Am. Chem. Soc.* **2003**, 125, 9560.

Scheme 1. Synthesis of 1^a



^a Reagents and conditions: (i) [Y{N(SiMe₃)₂}₃], toluene, 353 K, 20 h, 10%.

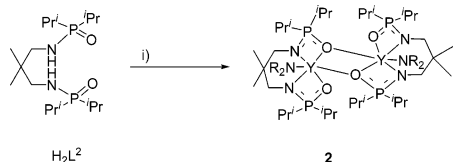
Hydroamination requires a catalyst with a Lewis acidic metal center and a metal amido bond of sufficient lability to allow insertion reactions. These catalyst requirements parallel those for lactide ring-opening polymerization initiators. Inspired by this observation, we discovered [Y{N(SiMe₃)₂}₃]{bis(trimethylsilyl)amido}-yttrium] was a highly active initiator for lactide ring-opening polymerization.¹⁹ Herein, we expand upon these promising preliminary results and report the syntheses, structures, and ring-opening polymerization activities of a series of [Y{N(SiMe₃)₂}₃]{bis(*P,P'*-di-isopropoxyphosphonic)-2,2-dimethylpropylenediamido}-[amido]yttrium] complexes.

Results and Discussion

[Y{N(SiMe₃)₂}₃]{bis(*P,P'*-di-isopropylthiophosphonic)-2,2-dimethylamido}{bis(trimethylsilyl)amido}yttrium], **1**. The yttrium amido complex **1** was prepared by an amine elimination route via the reaction of *N,N'*-1,3-bis(*P,P'*-di-isopropylthiophosphonic)-2,2-dimethylpropylenediamine (H₂L¹) with [Y{N(SiMe₃)₂}₃], as shown in Scheme 1.

H₂L¹ was synthesized by the reaction of 2 equiv of di(isopropyl)thiophosphonic chloride⁴⁰ with 2,2-dimethylpropylene-1,3-diamine. It was isolated as a white powder in good yield and analytical purity. The yield was improved using this novel route, as it prevented the competitive oxidation reaction and eliminated the need for ligand purification via column chromatography.³⁹ Initially, the reaction between H₂L¹ and [Y{N(SiMe₃)₂}₃] was conducted at 353 K in toluene and provided a low yield (10%) of **1**. The X-ray crystal structure (Figure S1) of **1** shows a square-planar coordination geometry at the yttrium with the tetradentate ligand occupying the basal coordination sites and the amide group occupying the apical site.¹⁹ The complex was a highly active and controlled initiator for lactide polymerization; it had a propagation rate constant (*k_p*) of 0.19 M⁻¹ s⁻¹, which is among the largest yet reported and orders of magnitude greater than many other homo-/heteroleptic yttrium amido complexes. However, the synthesis of the complex was problematic, as the isolated yield was low and it readily decomposed on heating. Indeed such solvent effects have also been observed by others working with “soft” donor substituted diamides.^{23,27} The synthesis was improved by using THF as the solvent; it was monitored using ³¹P{¹H} NMR spectroscopy, which indicated complete conversion to a single product after 7 days stirring at room temperature. The ³¹P{¹H} NMR spectrum showed a doublet at 72.60 ppm with a coupling constant of 5.36 Hz due to coupling with the ⁸⁹Y. The magnitude of the coupling constant, the multiplicity, and the chemical shift of **1** were consistent with the spectra obtained by Ibers et al. for homoleptic tris(thio-/selenophosphoramido)yttrium com-

(40) Birdsall, D. J.; Slawin, A. M. Z.; Woollins, J. D. *Polyhedron* **2001**, 20, 125.

Scheme 2. Synthesis of 2^a

^a Reagents and conditions: (i) $[\text{Y}\{\text{N}(\text{SiMe}_2\text{H})_2\}_3 \cdot 2\text{THF}]$, toluene, 20 h, 298 K, 74%. R = SiMe_2H .

plexes.⁴¹ The ¹H NMR spectrum showed integrals for the ligand and amide protons consistent with formation of an $[\text{L}^1\text{Y}(\text{N}(\text{SiMe}_3)_2)_2]$ complex. The mononuclear solution structure was confirmed using ¹H PGSE NMR experiments (see Experimental Section), which gave a solution hydrodynamic radius, for **1** in THF, of 5.27 Å, which was in excellent agreement with the value of 5.15 Å calculated from the X-ray crystal structure.⁴²

$[\{N,N'-1,3\text{-Bis}(P,P'\text{-di-isopropoxyphosphinic})\text{-}2,2\text{-dimethylpropylenediamido}\}\{\text{amido}\}\text{yttrium}]$ Complexes 2–4.

In order to investigate the influence of the neutral donor atom on the coordination chemistry and lactide polymerization activity, bis(oxophosphinic)diamido yttrium complexes were also synthesized. Livinghouse et al. previously tested $N,N'-1,3\text{-bis}(P,P'\text{-diphenyloxophosphinic})\text{-}2,2\text{-dimethylpropylenediamine}$ for *in situ* hydroamination activity with $[\text{Y}\{\text{N}(\text{SiMe}_3)_2\}_3]$, but the system showed much lower activity than using bis-(thiophosphinic)diamine ligands.³⁹ Recently, Bergmann and co-workers reported some highly active hydroamination catalysts prepared *in situ* by reaction of various bis(P,P' -diaryloxophosphinic)diamines and $[\text{Zr}(\text{NMe}_2)_4]$.⁴³ In this study it was relevant to contrast the influence of the harder O-donor ligands with the softer S-donor ligands on the coordination chemistry and ROP activity of the yttrium complexes. As **1** had previously shown such good lactide polymerization activity, the analogous O-substituted ligand $N,N'-1,3\text{-bis}(P,P'\text{-di-isopropoxyphosphinic})\text{-}2,2\text{-dimethylpropylenediamine}$ (H_2L^2) was targeted. H_2L^2 was prepared in good yield and analytical purity using an adaptation of the method reported by Bergmann et al. for related diaryl-substituted ligands.⁴³ The coordination chemistry was undertaken according to the extended silylamide methodology,⁴⁴ as shown in Scheme 2, by combining H_2L^2 and $[\text{Y}\{\text{N}(\text{SiMe}_2\text{H})_2\}_3 \cdot 2\text{THF}]$.

The complexation reaction was monitored by ³¹P{¹H} NMR spectroscopy, which showed complete consumption of H_2L^2 and formation of **2** after 20 h stirring at room temperature. The ¹H NMR spectrum also showed the disappearance of the N–H signals and the formation of **2** equiv of bis(dimethylsilyl)amine. The complex was isolated in 74% yield as a white solid; its elemental analysis was in excellent agreement with the formation of a chelating complex **2** with stoichiometry $[\text{L}^2\text{YN}(\text{SiMe}_2\text{H})_2]$.

Solid-State Structure: X-ray Crystallography. Crystals of **2** suitable for X-ray analysis were grown from a toluene solution, and the solid-state structure shows the complex to be an unexpected dinuclear species (Figure 1), each of the two L^2 ligands making four bonds to one metal center and one to the other. The two ends of the symmetric L^2 ligands are therefore

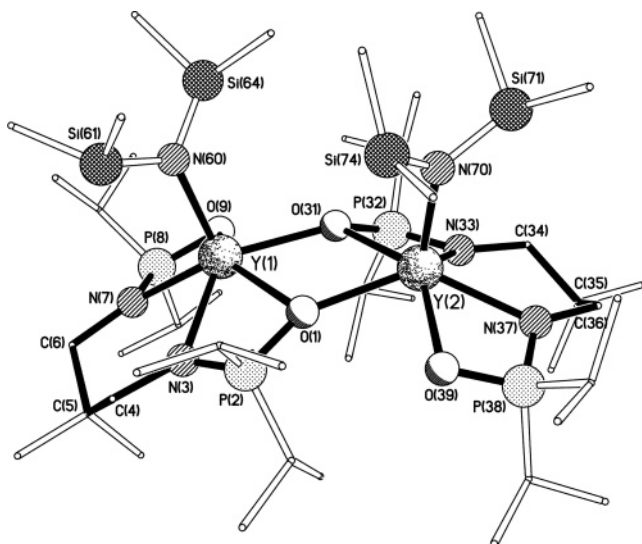


Figure 1. Molecular structure of **2**.

different; while O(9) and O(39) are each bonded to just one yttrium atom, O(1) and O(31) bridge between the two metal centers, forming a central Y_2O_2 ring. The two yttrium atoms both have a distorted pentagonal pyramidal coordination geometry with a bis(dimethylsilyl)amido ligand occupying the apical site. However, while the basal plane for Y(1) is coplanar to within ca. 0.04 Å [the metal lying ca. 0.61 Å out of this plane in the direction of the apical ligand], the basal plane at Y(2) is only coplanar to within ca. 0.16 Å [Y(2) lying ca. 0.67 Å out of this plane], and in fact the O(31) center lies ca. 0.38 Å out of the plane of the remaining four atoms of the basal plane [which are coplanar to within ca. 0.02 Å]. The two N_2O_3 basal planes are inclined by ca. 29° to each other, with the two apical ligands being on the same “outer” face of this folded molecule such that the $\text{N}(60)\cdots\text{N}(70)$ separation of 5.189(11) Å is substantially larger than the $\text{Y}(1)\cdots\text{Y}(2)$ separation of 4.0472(17) Å. The central four-membered Y_2O_2 ring is folded in the opposite sense about the $\text{O}(1)\cdots\text{O}(31)$ vector by ca. 9°, Y(2) lying ca. 0.30 Å out of the $\{\text{Y}(1), \text{O}(1), \text{O}(31)\}$ plane in the direction of N(70);⁴⁵ the transannular $\text{O}(1)\cdots\text{O}(31)$ separation is 2.691(6) Å. The Y–O bonds within the ring are noticeably asymmetric (Table 2) with those that are part of the NPOY chelate rings [$\text{Y}(1)\text{—O}(1)$ 2.524(5) Å, $\text{Y}(2)\text{—O}(31)$ 2.585(5) Å], more than 0.2 Å longer than the other two [$\text{Y}(1)\text{—O}(31)$ 2.312(5) Å, $\text{Y}(2)\text{—O}(1)$ 2.307(5) Å]. These latter bond lengths are very similar to the Y–O bonds of the other NPOY chelate ring formed by each of the two tetradentate ligands (i.e., the ring that is not involved in joining the two metal centers) [$\text{Y}(1)\text{—O}(9)$ 2.315(5) Å, $\text{Y}(2)\text{—O}(39)$ 2.320(5) Å], suggesting that it is the $\text{Y}(1)\text{—O}(1)$ and $\text{Y}(2)\text{—O}(31)$ bonds that are anomalously long. The two Y–N(SiMe_2H)₂ distances here in **2** differ by ca. 0.04 Å [$\text{Y}(1)\text{—N}(60)$ 2.216(6) Å, $\text{Y}(2)\text{—N}(70)$ 2.253(7) Å], and an even greater difference is seen between the $\text{Y}(1)\text{—O}(1)$ [2.524(5) Å] and $\text{Y}(2)\text{—O}(31)$ bonds [2.585(5) Å]. The reasons for these differences are not immediately apparent, but may be linked to the greater distortion seen in the basal plane around Y(2) compared to that around Y(1) (*vide supra*). The geometries of the four NPOY chelate rings fall into two categories, with the two involved in the bridging between the two metal centers being much more folded [P(2) and P(32) lie ca. 0.20 and 0.09 Å out of their respective YNO planes] than the others [P(8) and P(38) lie ca. 0.05 and 0.01 Å out of

(41) Pemin, C. G.; Ibers, J. A. *Inorg. Chem.* **2000**, *39*, 1222.

(42) The packing index (percentage of filled space in the unit cell) was calculated from the X-ray crystal structure. This packing index was used to calculate the volume of one molecule, and the molecule was assumed to be spherical. The X-ray hydrodynamic radius was determined using the equation for the volume of a sphere.

(43) Watson, D. A.; Chiu, M.; Bergmann, R. G. *Organometallics* **2006**, *25*, 4731.

(44) Runte, O.; Priermeier, T.; Anwender, R. *Chem. Commun.* **1996**, 1385.

(45) This fold can also be viewed as Y(1) lying ca. 0.30 Å out of the $\{\text{Y}(2), \text{O}(1), \text{O}(31)\}$ plane in the direction of N(60).

Table 1. Selected Bond Lengths (Å) and Angles (deg) for **2**

bond	length	bond	length
Y(1)–O(1)	2.524(5)	Y(1)–N(3)	2.359(6)
Y(1)–N(7)	2.345(6)	Y(1)–O(9)	2.315(5)
Y(1)–O(31)	2.312(5)	Y(1)–N(60)	2.216(6)
Y(2)–O(1)	2.307(5)	Y(2)–O(31)	2.585(5)
Y(2)–N(33)	2.329(6)	Y(2)–N(37)	2.343(6)
Y(2)–O(39)	2.320(5)	Y(2)–N(70)	2.253(7)

bond	angle	bond	angle
O(1)–Y(1)–N(3)	60.01(18)	O(1)–Y(1)–N(7)	132.23(18)
O(1)–Y(1)–O(9)	140.75(16)	O(1)–Y(1)–O(31)	67.46(15)
O(1)–Y(1)–N(60)	105.6(2)	N(3)–Y(1)–N(7)	75.4(2)
N(3)–Y(1)–O(9)	132.0(2)	N(3)–Y(1)–O(31)	123.56(18)
N(3)–Y(1)–N(60)	109.7(2)	N(7)–Y(1)–O(9)	62.7(2)
N(7)–Y(1)–O(31)	137.9(2)	N(7)–Y(1)–N(60)	104.7(2)
O(9)–Y(1)–O(31)	80.42(17)	O(9)–Y(1)–N(60)	102.9(2)
O(31)–Y(1)–N(60)	102.6(2)	O(1)–Y(2)–O(31)	66.48(15)
O(1)–Y(2)–N(33)	117.3(2)	O(1)–Y(2)–N(37)	134.26(18)
O(1)–Y(2)–O(39)	79.67(17)	O(1)–Y(2)–N(70)	109.5(2)
O(31)–Y(2)–N(33)	59.83(17)	O(31)–Y(2)–N(37)	133.05(19)
O(31)–Y(2)–O(39)	141.93(17)	O(31)–Y(2)–N(70)	105.60(19)
N(33)–Y(2)–N(37)	74.8(2)	N(33)–Y(2)–O(39)	129.7(2)
N(33)–Y(2)–N(70)	113.9(2)	N(37)–Y(2)–O(39)	62.78(19)
N(37)–Y(2)–N(70)	103.2(2)	O(39)–Y(2)–N(70)	101.6(2)
Y(1)–O(1)–Y(2)	113.74(18)	Y(1)–O(31)–Y(2)	111.36(17)

Table 2. $^{31}\text{P}\{^1\text{H}\}$ NMR Signals for Complexes **2–4**

complex	H_2L^2 chemical shift, δ ppm (multiplicity) ^a	complex chemical shift, δ ppm (multiplicity, integral) ^a
2	52.4 (s)	major: 67.1 (ddd, 13P), 55.1 (dd, 13P) minor: 69.0 (m, 1P), 56.9 (m, 1P)
3	52.4 (s)	65.4 (ddd, 1P), 57.1 (dd, 1P)
4	52.4 (s)	61.8 (ddd, 1P), 57.1 (dd, 1P)

^a The spectra were obtained in d_6 -benzene.

their respective YNO planes]. The two $\text{C}_3\text{N}_2\text{Y}$ six-membered chelate rings have flattened chair conformations; for the N(3)/N(7) ring, Y(1) and C(5) lie ca. +0.60 and –0.72 Å “above” and “below” the {N(3),C(4),C(6),C(7)} plane, respectively (which is coplanar to within better than 0.01 Å), and for the N(33)/N(37) ring, Y(2) and C(55) lie ca. +0.66 and –0.71 Å above and below the {N(33),C(34),C(36),C(37)} plane, respectively (which is coplanar to within better than 0.01 Å). The bottom face of the complex, though theoretically exposed, is actually obscured by the downwardly directed isopropyl groups on P(2), P(8), P(32), and P(38) and by the methyl groups on C(5) and C(35).

Solution Structure: NMR Spectroscopies. In order to understand the lactide polymerization results, it was essential to establish whether the dimeric structure was maintained in solution and in particular in non-coordinating solvents, as these were preferred for the polymerization.¹⁹ The ^1H NMR spectrum indicated complexation due to the disappearance of the NH signals at 3.20 ppm. It also showed an asymmetric L^2 coordination environment with the methylene groups splitting into two doublets of doublets, each integrating to one proton, and a multiplet, integrating to two protons. The methyl groups in the 2,2-dimethylpropyl backbone were also split into two singlets, each integrating to three. The phosphorus isopropyl substituents were inequivalent, as indicated by the four methine septets, each integrating to one; the two methyl group doublets of doublets, each integrating to three; and the two methyl group multiplets, each integrating to nine. The resonance for the amido group Si–H was a clear indicator of coordination, shifting from 5.00 ppm in $\text{Y}[\text{N}(\text{SiHMe}_2)_2]_3 \cdot 2\text{THF}$ to a multiplet at 5.19 ppm in **2**, consistent with the increased deshielding experienced on complexation. The amido methyl groups were two doublets, each

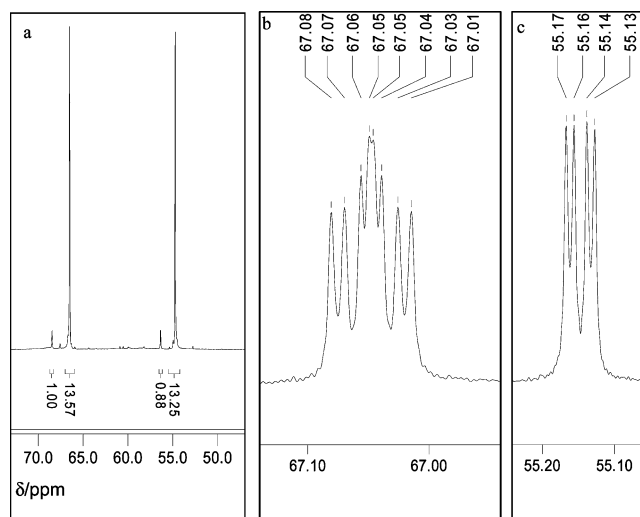


Figure 2. $^{31}\text{P}\{^1\text{H}\}$ NMR spectra of complex **2** in toluene- d_8 . (a) The entire spectrum showing two major peaks (67.1 and 55.1 ppm) and two minor peaks (69.0 and 56.9 ppm). (b) The peak centered at 67.1 ppm (ddd, $^2J_{\text{PY}} = 5.10, 3.97$ Hz; $^4J_{\text{PP}} = 1.78$ Hz). (c) The peak centered at 55.1 ppm (dd, $^2J_{\text{PY}} = 4.65$ Hz; $^4J_{\text{PP}} = 1.76$ Hz).

integrating to six, indicative of restricted rotation about the Y–N bonds. Such restricted bond rotation has been previously observed at low temperature by Bradley et al. for (trimethylphosphineoxide)tris(bis(trimethylsilyl)amido)lanthanide complexes⁴⁶ and recently by Hill et al. at room temperature for a bis(iminophosphonamido)(bis(dimethylsilylamido))yttrium complex.³⁵ The $^{13}\text{C}\{^1\text{H}\}$ NMR also showed the restricted rotation, with the amido methyl carbons resonating at 4.8 and 4.4 ppm. The asymmetric coordination environment for L^2 was also confirmed by the two methylene and two methyl carbon signals for the 2,2-dimethylpropylene backbone and by the four methine and six methyl carbon signals for the isopropyl phosphorus substituents. While the ^1H and $^{13}\text{C}\{^1\text{H}\}$ NMR spectra indicated the stoichiometry of **2**, they did not confirm the precise solution structure. The $^{31}\text{P}\{^1\text{H}\}$ NMR spectrum showed the disappearance of the H_2L^2 resonance, at 52.4 ppm, and the evolution of four new resonances at 67.1 and 55.1 ppm, each of equal integration, and two minor peaks at 69.0 and 56.9 ppm, also of equal integration. The relative integration of the major to minor peaks was 13:1. $^{31}\text{P}\{^1\text{H}\}$ NMR inverse gated experiments (see Experimental Section) showed the true multiplicity of the signals (Figure 2b,c). Thus, the major peak at 55.1 ppm was a doublet of doublets, with coupling constants of 4.65 and 1.76 Hz, while the peak at 67.1 ppm was a doublet of doublets of doublets, with coupling constants of 5.10, 3.97, and 1.78 Hz. The resolution of the minor peaks' coupling was not possible due to their low intensity. The NMR spectra indicated the dimeric solid-state structure was maintained in solution with one oxophosphinic group bridging between two yttrium centers and the other bonding to just one yttrium center. Thus, the resonance at 67.1 ppm was assigned to the phosphorus of the bridging oxophosphinic group. In the solid state it was asymmetrically bonded to the two yttriums, and this was maintained in solution, where two $^3J_{\text{PY}}$ couplings of 5.10 and 3.97 Hz were observed. The relative magnitudes of the coupling constants reflect the lengths of the Y–O bonds, which were 2.52 and 2.31 Å in the X-ray crystal structure. Furthermore, the magnitudes of the coupling constants were consistent with the values obtained by Ibers et al. for homoleptic

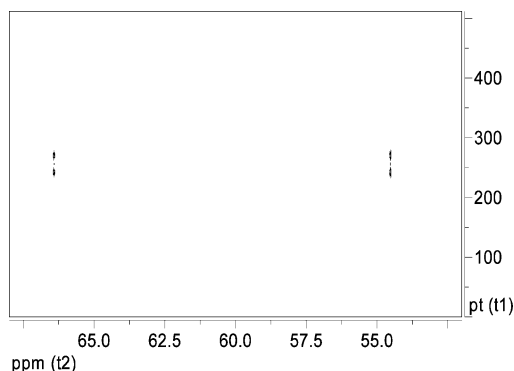


Figure 3. 2D J -resolved $^{31}\text{P}\{^1\text{H}\}$ NMR spectrum of **2**; $^4J_{\text{PP}} = 1.75$ Hz.

tris(thiophosphinic amido)yttrium complexes and also with the coupling constant for **1**.⁴¹ The coupling of 1.78 Hz was assigned to $^4J_{\text{PP}}$ coupling. The doublet of doublets at 55.1 ppm was assigned to the phosphorus nuclei of the oxophosphinic group bonded to just one yttrium. It showed a $^3J_{\text{YP}}$ of 4.65 Hz and a $^4J_{\text{PP}}$ of 1.76 Hz. The 2D J -resolved $^{31}\text{P}\{^1\text{H}\}$ NMR experiment confirmed the $^4J_{\text{PP}}$ homonuclear coupling between the resonances at 55.1 and 67.1 ppm (Figure 3).

A ^1H pulsed gradient spin echo (PGSE) experiment was used to determine the solution diffusion coefficient for **2**. This method has been previously used to investigate monomer–dimer equilibria.^{47,48} Using the Stokes–Einstein equation, the diffusion coefficient, obtained from the PGSE experiments, was related to the hydrodynamic radius. The PGSE experiment gave a radius of 6.46 Å for **2**, which fits very favorably with the radius of 6.28 Å obtained from the X-ray crystal structure, indicating that **2** exists as a dimer in solution.⁴² Overall, the NMR experiments suggested a dimeric solution structure, with two isomers being present in a ratio of 13:1 at room temperature. Attempts to investigate the isomerization by VT-NMR were inconclusive due to the high noise at elevated temperatures and the low intensity of the minor isomer's signals. The isomerization is probably related to the conformation of the bis(dimethylsilyl)-amido group, the L^2Y chelate ring conformation, and/or the yttrium coordination geometry. An agostic interaction between the Si–H and the yttrium center was ruled out by the IR spectrum, which showed Si–H stretches at 2089 and 2044 cm^{-1} (agostic interactions are characterized by Si–H stretches at 1700–1800 cm^{-1}).⁴⁹

Amido Group Substitution. The influence of the amido group on the structure of the yttrium complex was probed by changing the yttrium precursor complex, and some novel dimeric complexes were synthesized (Figure 4).

H_2L^2 was reacted with three different homoleptic tris(amido)-yttrium precursors in toluene at room temperature over several hours. The reactions were monitored by $^{31}\text{P}\{^1\text{H}\}$ NMR spectroscopy, which showed the disappearance of the H_2L^2 signal and the growth of the complexes' resonances. There was no evidence for formation of any other intermediate complexes. Upon complete consumption of the H_2L^2 resonance, the solvents were evaporated to remove the liberated amine; **3** took significantly longer to form (48 h vs 20 h for **2** and **4**) due to

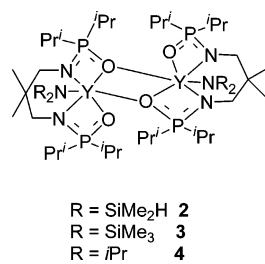


Figure 4. Structures of complexes **2–4**.

the increased steric bulk of the tris(amido)yttrium precursor. The complexes were isolated as white powders, all showing excellent agreement between the calculated and experimental elemental analyses. The $^{31}\text{P}\{^1\text{H}\}$ NMR spectra were closely related to that obtained for **2** and indicated formation of dimeric structures with the oxophosphinic groups occupying terminal and bridging coordination geometries (Table 2).

Both **3** and **4** showed two multiplets in the $^{31}\text{P}\{^1\text{H}\}$ NMR spectra: a doublet of doublets of doublets due to the bridging oxophosphinic group and at higher field a doublet of doublets due to the terminal oxophosphinic group. Changing either the size or the relative acidity of the amido group does not influence the structure of the complex formed; however, it is noteworthy that only **2** showed the formation of two different sets of isomers. The ^1H NMR spectra for both **3** and **4** were consistent with dimeric solution structures. The 2,2-dimethylpropylene backbone showed four doublets of doublets due to the methylene protons and two singlets for the methyl protons. The phosphorus isopropyl substituents gave four distinct septets for the methine protons and eight doublets for the methyl protons. Furthermore, both **3** and **4** showed restricted rotation about the Y–N bond, on the ^1H NMR time scale, with two singlets for the bis-(trimethylsilyl)amido protons on **3** and two doublets for the di-(isopropyl)amido protons on **4**. The $^{13}\text{C}\{^1\text{H}\}$ NMR spectra for **3** and **4** also confirmed the dimeric structures with separate resonances for the methylene and methyl carbons of the 2,2-dimethylpropylene backbone and for the methine and methyl carbons of the isopropyl phosphorus substituents. The slow rotation about the Y–N bond (on the NMR time scale) led to two methyl carbon signals for the substituents on the amido groups on both **3** and **4**.

Lactide Ring-Opening Polymerization (ROP). The new yttrium complexes **1–4** were investigated as initiators for *rac*-lactide ROP. The properties of monomeric [$\text{L}^1\text{Y}(\text{NR}_2)$] and dimeric [$\text{L}^2\text{Y}(\text{NR}_2)$]₂ complexes were contrasted using **1** and **2**, with various solvents and at different concentrations (Table 3).

The polymerizations all went to complete conversion in a very rapid time, and **2** was an even faster initiator than **1**. Thus, at 10 mM initiator concentration (for **2** this refers to the concentration of the $\text{N}(\text{SiMe}_2\text{H})_2$ initiating groups), 99% conversion was achieved for **2** in only 70 s compared to 360 s for **1**. The polymerizations in THF were slower than in methylene chloride. The diminution in rate was attributed to competitive binding of the yttrium by the coordinating solvent. The polymerization control exerted by monomeric **1** was excellent, with close agreement between the calculated and experimental M_n ; however, dimeric **2** had a poor correlation between the experimental and calculated M_n . For **2**, the evolution of M_n with % conversion (Figure 5) showed a linear fit, as expected for a controlled polymerization; however, the M_n values were approximately twice the calculated values throughout the polymerization run. The M_n data were consistent with **2** retaining its dimeric structure during the polymerization, but

(47) Geldbach, T. J.; Pregosin, P. S.; Albinati, A.; Rominger, F. *Organometallics* **2001**, *20*, 1932.

(48) Williams, C. K.; Breyfogle, L. E.; Choi, S. K.; Nam, W. W.; Young, V. G., Jr.; Hillmyer, M. A.; Tolman, W. B. *J. Am. Chem. Soc.* **2003**, *125*, 11350.

(49) Hermann, W. A.; Eppinger, J.; Spiegler, M.; Runte, O.; Anwender, R. *Organometallics* **1997**, *16*, 1813.

Table 3. Percent Conversions, Times, M_n , and PDI Obtained Using Initiators **1** and **2**

solvent ^a	initiator	[initiator] ₀ /mM	time/s	% conversion ^c	M_n /kg mol ⁻¹ (PDI) ^d	M_n calcd/kg mol ^{-1 e}
CH ₂ Cl ₂	1	10	360	94	17.9 (1.60)	14.4
CH ₂ Cl ₂	1	2	960	74	50 (1.60)	53.0
THF	1	5	1080	90	26.0 (1.40)	27.8
CH ₂ Cl ₂	2	10	70	98	40.8 (1.84)	14.4
CH ₂ Cl ₂	2	5	221	99	66.4 (1.68)	28.8
CH ₂ Cl ₂	2	3.3	300	99	78.6 (1.64)	43.2
CH ₂ Cl ₂	2	2	700	46	74.3 (1.49)	33.1
THF	2	5	372	88	56.1 (1.74)	25.3

^a Polymerization conditions: [lactide]₀ = 1 M, 298 K. ^b[initiator]₀ = [**1**], but for **2**, **3**, **4** [initiator]₀ = [NR₂]₀ (i.e., 2 × [2/3/4]₀). ^cDetermined by integration of the methine region of the ¹H NMR spectrum. ^dDetermined by SEC in THF vs polystyrene standards and using a correction factor of 0.58.⁵⁵ ^e M_n calculated = (144 × [initiator/mM]₀ × 10 × % conversion).

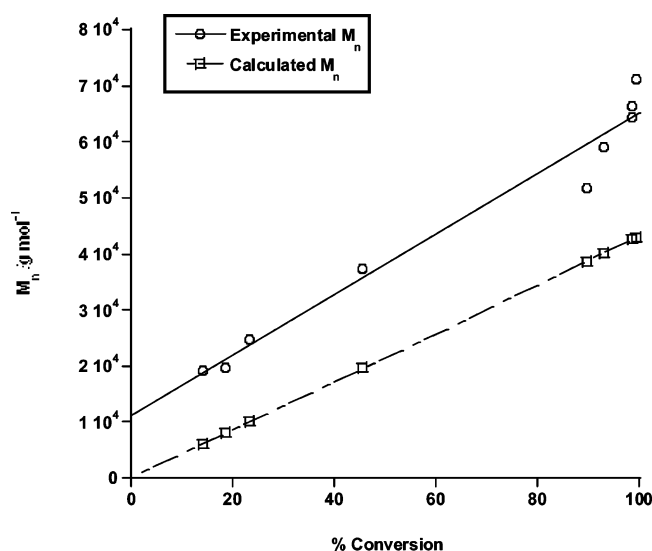


Figure 5. Plot showing M_n vs % conversion for **2**. Polymerization conditions: [lactide]₀ = 1 M, [N(SiMe₂H)₂]₀ = 2 mM in CH₂Cl₂ at 298 K. M_n calculated = (144 × [N(SiMe₂H)₂/mM]₀ × 10 × % conversion).

Table 4. Lactide ROP Using Initiators **2–4** (polymerization conditions: [lactide]₀ = 1 M, [NR₂]₀ = 5 mM in CH₂Cl₂ at 298 K)

initiator	% conversion ^a	time/s	M_n ^b	PDI
2	99	221	66.4	1.68
3	99	74	85.8	1.71
4	98	158	22.2	1.77

^a Determined by integration of the methine region of the ¹H NMR spectrum. ^bDetermined by SEC in THF vs polystyrene standards and using a correction factor of 0.58.⁵⁵

with only one of its amide groups initiating the polymerization, probably due to the relatively large size and close proximity of the two bis(dimethylsilylamido) groups.⁵⁰ Indeed, the dimeric structure adopted by **2** was remarkably stable and inert; for example, addition of several equivalents of THF or pyridine to toluene solutions of **2** did not change its NMR spectra.

The complexes **2–4**, differing in their amido group substituents, were compared as initiators for lactide ROP (Table 4). The polymerizations were conducted in methylene chloride at room temperature, as these were the optimum conditions for **2**.

All three initiators showed extremely rapid lactide polymerization. It is notable that the times required for complete lactide conversion are significantly faster than those obtained with other

heteroleptic yttrium amido complexes, including **1**.^{15–21} Furthermore, **2–4** do not undergo any redistribution reactions under the polymerization conditions, as the homoleptic tris(amido)-yttrium complexes typically took hours to go to complete conversion under the same polymerization conditions.

The M_n values observed using initiators **2** and **3** were approximately double the calculated values, but **4** showed a very good correlation between the calculated and observed M_n . The greater steric bulk of the amido substituents on **2** and **3** (trimethylsilyl and dimethylsilyl) compared to **4** (isopropyl) was proposed to prevent initiation from both amide groups, leading to M_n values double those calculated on the basis of amide group concentration. This notion was supported by ¹H NMR monitoring of the reaction of **2** with 2 equiv of lactide, which showed two Si–H resonances, one at the same chemical shift as **2** and the other at lower field assigned to the amide end group on the ring-opened lactide. These methyl group resonances were consistent with only one amide group on each dimer reacting with lactide. Furthermore, the ³¹P{¹H} NMR spectrum for the reaction of **2** with 2 equiv of lactide showed the same four resonances as observed for **2**, indicating that the dimeric structure was maintained during initiation. On the other hand, it is proposed that the less hindered amide groups on **4** were both able to initiate lactide ROP, leading to M_n in excellent agreement with those calculated on the basis of amide group concentration.

For all the initiators, the homonuclear decoupled ¹H NMR spectra of the PLA showed isotactic PLA was produced from *S*-lactide; that is, there were no epimerization side reactions occurring. The PLA produced from *rac*-lactide showed a slight heterotactic bias with *P_s* values of 0.61–0.64. The tacticity was not changed either at lower conversions or by using coordinating solvents.

All three initiators showed relatively large polydispersity indices (PDI) for the PLA. This was probably due to the very fast rates of polymerization, which resulted in a lower value for $k_{\text{initiation}}/k_{\text{propagation}}$, as has been found for other amide initiating groups, and/or to intermolecular transesterification side reactions. The polymerization kinetics for **2–4** were complex, with the initiators showing ln[LA]₀/[LA]_{*t*} versus time plots that were nonlinear (Figure S3). Such nonlinear plots prevent any direct comparison of the k_{obs} values with **1**. We are currently carrying out detailed investigations to establish the polymerization kinetics, mechanism for stereocontrol, and structures of the propagating complexes.

Conclusions

In conclusion, the synthesis and characterization of a series of novel [{*N,N'*-1,3-bis(*P,P'*-di-isopropoxythiophosphinic)-2,2-dimethylpropylenediamido}(amido)yttrium] complexes have

(50) An alternative explanation where **2** undergoes slow equilibration to a mononuclear active initiator cannot be discounted at this stage.

been described. The complexes were synthesized by an amine elimination route from $[Y(NR_2)_3 \cdot xTHF]$ precursors (where $R = SiMe_3, SiMe_2H,$ and $i-Pr, x = 0, 2$) with the ligands H_2L^1 or H_2L^2 . The synthetic yields were excellent, and the new compounds were characterized by X-ray crystallography, elemental analysis, and IR and NMR spectroscopies. The $[N,N'-1,3-bis(P,P'-di-isopropylthiophosphinic)-2,2-dimethylpropylenediamido]\{bis(trimethylsilyl)amido\}yttrium$ complex was monomeric in both the solid state and solution, as established by X-ray crystallography and PGSE NMR experiments. In contrast, the $[N,N'-1,3-bis(P,P'-di-isopropylloxophosphinic)-2,2-dimethylpropylenediamido]\{amido\}yttrium$ complexes showed unusual dimeric structures, with each ligand coordinating to a single yttrium center via a terminal oxophosphinic group and coordinating to two yttrium centers via a bridging oxophosphinic group. The X-ray crystal structure for one of these complexes was reported, and the dimeric solution structure was established using a variety of NMR techniques. All the new complexes were tested as lactide ROP initiators, and all showed very high rates and reasonable degrees of control. The dimeric complexes with bis(dimethylsilyl)amido and bis(trimethylsilyl)amido groups displayed poor correlations between M_n observed and that calculated from the reaction stoichiometry, consistent with only one of the two amido groups initiating the polymerization. However, the dimeric complex with smaller di(isopropyl)amido groups showed a good correlation between the calculated and observed M_n , consistent with initiation from both amido groups. These novel yttrium complexes therefore display promise as a new type of highly active and controlled initiator for lactide ring-opening polymerization. The detailed study of their kinetics and mechanism is currently underway and will be reported in due course.

Experimental Section

Materials and Methods. All reactions were conducted under a nitrogen atmosphere, either using standard anaerobic techniques or in a nitrogen-filled glovebox. All solvents and reagents were obtained from commercial sources (Aldrich and Merck) and dried. Tetrahydrofuran and toluene were distilled from sodium and stored under nitrogen. Deuterated solvents were dried by stirring them with either calcium hydride (dichloromethane- d_2 , chloroform- d_3) or potassium (tetrahydrofuran- d_8 , toluene- d_8 , benzene- d_6), performing three freeze–thaw cycles under vacuum, refluxing them for 1–2 days, distilling them under vacuum, and storing them under nitrogen. *rac*-Lactide was generously donated by Purac Plc. and was recrystallized from anhydrous ethyl acetate and sublimed three times under vacuum prior to use. Chloro di-isopropylthiophosphine,⁴⁰ $[Y\{N(SiMe_3)_2\}_3]$,⁵¹ $[Y\{N(SiHMe_2)_2\}_3 \cdot 2THF]$,⁵² and $[Y(Ni-Pr)_2 \cdot 2THF]$ ⁵³ were prepared according to literature procedures.

Measurements. 1H and ^{13}C NMR spectra were performed on a Bruker Av-400 instrument, unless otherwise stated. ^{31}P NMR experiments and 1H PGSE experiments were performed on a Bruker Av500 spectrometer equipped with a z-gradient bbo/5 mm tunable probe and a BSMS GAB 10 amp gradient amplifier, providing a maximum gradient output of 5.35 G/cmA. To observe the complex P–P coupling patterns, $^{31}P\{^1H\}$ spectra were collected at a frequency of 202.47 MHz using a 30° pulse, a spectral width of 8082 Hz (centered on 57.5 ppm), and 65 536 data points with a relaxation delay of 2 s. The spectra were zero filled (0.12 Hz/point resolution) and processed with no apodization.

The 1H PGSE (dosy) experiments were conducted according to the first literature procedure.⁵⁴ The spectra were collected at a frequency of 500.13 MHz with a spectral width of 4500 Hz (centered on 3.5 ppm) and 16 384 data points. A relaxation delay of 1 s was employed along with a diffusion time (Δ) of 50 ms and longitudinal eddy current delay (LED) of 5 ms. Bipolar gradient pulses ($\delta/2$) of 2.2 ms and homospoil gradient pulses of 1.1 ms were used. The gradient strengths of the 2 homospoil pulses were -17.13% and -13.17% . Thirty-two experiments were collected with the bipolar gradient strength initially at 2% (first experiment) and linearly increased to 95% (32nd experiment). All gradient pulses were sine shaped, and after each application a recovery delay of 200 μs was used. The spectra were zero filled and processed using an exponential function with a line broadening of 2 Hz. Further processing was achieved using the Bruker dosy software. Elemental analyses were determined by Mr. Stephen Boyer at London Metropolitan University, North Campus, Holloway Rd., London, N7. SEC data were collected using a Polymer Labs PL GPC-50 instrument with THF as the eluent, at a flow rate of 1 mL min⁻¹. Two Polymer Labs Mixed D columns were used in series, and the M_n were calibrated against narrow M_n polystyrene standards (Easy-Cal standards A and B). The values were corrected according to the literature.⁵⁵

$N,N'-1,3-Bis(P,P'-di-isopropylthiophosphinic)-2,2-dimethylpropylene diamine H_2L^1$.³⁹ 2,2-Dimethylpropylene-1,3-diamine (0.85 g, 8.32 mmol) and di-isopropylethylamine (3.35 mL, 19.20 mmol) were dissolved in CH_2Cl_2 (20 mL), and chlorodi-isopropylthiophosphine (2.60 mL, 8.32 mmol) was added. The solution was refluxed for 20 h, and a white precipitate formed that was filtered and washed with CH_2Cl_2 . The filtrate was concentrated *in vacuo* and the crude product recrystallized from a mixture of CH_2Cl_2 and pentane to yield the product as a white solid (2.00 g, 5.00 mmol, 60%).

1H NMR (400 MHz, C_6D_6) δ ppm: 2.92 (s, 4H, NCH_2), 2.78 (s, 2H, NH), 2.15 (spt, 4H, $^3J_{HH} = 7.20$ Hz, $CH(CH_3)_2$), 1.25–1.18 (dd, 24H, $^3J_{HH} = 6.8$ Hz, $CH(CH_3)_2$), 0.87 (s, 6H, $C(CH_3)_2$). $^{31}P\{^1H\}$ NMR (161.9 MHz, C_6D_6) δ ppm: 89.09. Anal. Calcd for $C_{17}H_{40}N_2P_2S_2$: C, 51.23, H, 10.12, N, 7.03. Found: C, 51.18, H, 10.13, N, 7.04.

$N,N'-1,3-Bis(P,P'-di-isopropylloxophosphinic)-2,2-dimethylpropylenediamine H_2L^2$. To a stirred solution of 2,2-dimethylpropylene-1,3-diamine (0.96 mL, 8 mmol) and di-isopropylethylamine (6.97 mL, 40 mmol) in CH_2Cl_2 (40 mL) was added chlorodi-isopropylphosphine (2.67 mL, 16.8 mmol), dropwise, via a syringe. The reaction mixture was stirred for 12 h, after which time it was opened to the atmosphere and cooled to 273 K. H_2O_2 (30% aqueous solution, 4.1 mL, 32 mmol) was added cautiously. After the addition, the reaction mixture was stirred for a further 10 min at 273 and at 298 K for 30 min, before being quenched with aqueous $Na_2S_2O_3$ (80 mL of a 1 M solution, 80 mmol). The layers were separated, and the aqueous layer was extracted with CH_2Cl_2 (3 \times 20 mL). The combined organic extracts were dried ($MgSO_4$) and the solvents removed *in vacuo* to give the title compound as colorless needles (1.47 g, 50%).

1H NMR (400 MHz, $CDCl_3$) δ ppm: 3.20 (m, 2H, NH), 2.81 (t, 4H, $^3J_{HH} = 8.0$ Hz, CH_2), 1.96 (d spt, 4H, $^2J_{P-H} = 9.2$ Hz, $^3J_{H-H} = 7.2$ Hz, $CH(CH_3)_2$), 1.18 (dd, 12H, $^3J_{P-H} = 5.6$ Hz, $^3J_{H-H} = 7.2$ Hz, $CH(CH_3)_2$), 1.14 (dd, 12H, $^3J_{P-H} = 5.6$ Hz, $^3J_{H-H} = 7.2$ Hz, $CH(CH_3)_2$), 0.85 (s, 6H, CH_3). $^{13}C\{^1H\}$ NMR (100 MHz, $CDCl_3$) δ ppm: 46.2 (s, CH_2), 37.0 (s, $C(CH_3)_2$), 26.5 (d, $^1J_{PC} = 81.0$ Hz, $CH(CH_3)_2$), 23.3 (s, CH_3), 16.2 (d, $^2J_{PC} = 2.1$ Hz, $CH(CH_3)_2$), 15.9 (d, $^2J_{PC} = 2.3$ Hz, $CH(CH_3)_2$). $^{31}P\{^1H\}$ NMR (162 MHz, $CDCl_3$) δ ppm: 54.0. IR (Nujol mull, NaCl) ν cm⁻¹: 3195 (m, N–H),

(51) Mu, Y.; Piers, W. E.; MacDonald, M. A.; Zaworotko, M. J. *Can. J. Chem.* **1995**, *73*, 2233.

(52) Lin, M. H.; RajanBabu, T. V. *Org. Lett.* **2002**, *4*, 1607.

(53) Aspinal, H. C.; Tillotson, M. R. *Polyhedron* **1994**, *13*, 3229.

(54) Wu, D.; Chen, A.; Johnson, C. S., Jr. *J. Magn. Reson. A* **1995**, *115*, 260.

(55) Kowalski, A.; Duda, A.; Penczek, S. *Macromolecules* **1998**, *31*, 2114.

1294 (w), 1273 (m, P=O), 1180 (m), 1146 (s). MS m/z (FAB⁺): 367 [M + H]⁺. Anal. Calcd for C₁₇H₄₀N₂O₂P₂: C, 55.72, H, 11.00, N, 7.64. Found: C, 55.66, H, 11.07, N, 7.56.

1.19 *N,N'*-1,3-Bis(*P,P'*-di-isopropylthiophosphinic)-2,2-dimethylpropylenediamine (100 mg, 0.25 mmol) and [Y{N(SiMe₃)₂}₃] (143 mg, 0.25 mmol) were dissolved in THF (3 mL). The reaction was stirred until the ligand peak had disappeared from the ³¹P{¹H} NMR (7 days). It was then ready to use as the initiator stock solution.

¹H NMR (400 MHz, C₆D₆O) δ ppm: 2.88 (m, 4H, CH₂) 2.33–2.04 (m, 4H, CH(CH₃)₂), 1.09–1.28 (m, 30H, 4 × CH(CH₃)₂, 2 × CH₃), 0.04 (s, 18H, Si(CH₃)₃). ³¹P{¹H} NMR (161.9 MHz, THF–CDCl₃ probe) δ ppm: 72.6 (d, ²J_{PY} = 5.36 Hz).

2. To a solution of tris[*N,N'*-bis(dimethylsilyl)amido]yttrium (0.13 g, 0.20 mmol) in toluene (2 mL) was added *N,N'*-1,3-bis(*P,P'*-di-isopropoxyphosphinic)-2,2-dimethylpropylenediamine (0.07 g, 0.20 mmol) in toluene (3 mL). The solution was stirred for 20 h, before the solvents were removed, *in vacuo*, to yield the product as a white solid (0.09 g, 74%).

¹H NMR (400 MHz, C₆D₆) δ ppm: 5.19 (m, 2H, SiH), 3.42 (dd, ²J_{HH} = 11.8 Hz, ³J_{HP} = 4.0 Hz, 1H, CH₂), 3.31 (dd, ²J_{HH} = 12.0 Hz, ³J_{HP} = 4.0 Hz, 1H, CH₂), 2.94 (m, 3H, CH₂ and CH(CH₃)₂), 2.32 (spt, ³J_{HH} = 7.2 Hz, 1H, CH(CH₃)₂), 2.24 (spt, ³J_{HH} = 6.8 Hz, 1H, CH(CH₃)₂), 1.78 (spt, ³J_{HH} = 6.4 Hz, 1H, CH(CH₃)₂), 1.50 (dd, ³J_{HH} = 7.2 Hz, ³J_{HP} = 15.2 Hz, 3H, CHCH₃), 1.41 (dd, ³J_{HH} = 7.2 Hz, ³J_{HP} = 15.8 Hz, 3H, CHCH₃), 1.23 (m, 9H, CH₃), 1.16 (s, 3H, CH₃), 1.05 (m, 9H, CHCH₃), 0.92 (s, 3H, CH₃), 0.49 (d, ³J_{HH} = 2.8 Hz, 6H, SiHCH₃), 0.47 (d, ³J_{HH} = 2.8 Hz, 6H, SiHCH₃). ¹³C{¹H} NMR (100 MHz, C₆D₆) δ ppm: 57.0 (s, CH₂), 56.4 (s, CH₂), 37.5 (s, C(CH₃)₂), 31.5 (d, ¹J_{CP} = 69.0 Hz, CH(CH₃)₂), 29.7 (d, ¹J_{CP} = 33.6 Hz, CH(CH₃)₂), 29.0 (d, ¹J_{CP} = 37.2 Hz, CH(CH₃)₂), 27.1 (s, CCH₃), 26.6 (d, ¹J_{CP} = 66.5 Hz, CH(CH₃)₂), 25.4 (s, CCH₃), 18.6 (s, CHCH₃), 17.7 (s, CHCH₃), 17.4 (s, CHCH₃), 17.2 (s, CHCH₃), 17.0 (s, CHCH₃), 16.4 (s, CHCH₃), 4.8 (s, SiCH₃), 4.4 (s, SiCH₃). ³¹P{¹H} NMR (162 MHz, C₆D₆) δ ppm: 69.0 (m, 1P), 67.1 (ddd, ²J_{PY} = 5.10, 3.97 Hz; ⁴J_{PP} = 1.78 Hz, 13P), 56.9 (d, ²J_{PY} = 4 Hz, 1H), 55.1 (dd, ²J_{PY} = 4.65 Hz; ⁴J_{PP} = 1.76 Hz, 13P). IR (Nujol mull, NaCl) ν cm⁻¹: 2089 (s, Si–H), 2044 (m, Si–H), 1599 (w), 1288 (m, Si–CH₃ deformation), 1263 (m, Si–CH₃ deformation), 1240 (s, P=O), 1223 (s, P=O), 1184 (m), 1165 (m), 1061 (s), 1012 (s). Anal. Calcd for C₁₈H₄₆N₃O₂P₂–Si₂Y: C, 39.77, H, 8.53, N, 7.73. Found: C, 39.82, H, 8.45, N, 7.88.

Crystal data for 2: C₄₂H₁₀₄N₆O₄P₄Si₄Y₂, *M* = 1171.37, triclinic, *P* $\bar{1}$ (no. 2), *a* = 11.231(2) Å, *b* = 13.701(3) Å, *c* = 23.177(5) Å, α = 102.79(2)°, β = 92.532(16)°, γ = 114.151(17)°, *V* = 3136.9(11) Å³, *Z* = 2, *D*_c = 1.240 g cm⁻³, μ(Cu Kα) = 4.469 mm⁻¹, *T* = 173 K, colorless plates, Oxford Diffraction Xcalibur PX Ultra diffractometer; 11 881 independent measured reflections, *F*² refinement, *R*₁ = 0.068, *wR*₂ = 0.197, 7624 independent observed absorption-corrected reflections [*I*(*F*_o) > 4σ(*I*(*F*_o))], 2θ_{max} = 142°], 559 parameters. CCDC 638409.

3. To a solution of tris[*N,N'*-bis(trimethylsilyl)amido]yttrium (0.09 g, 0.15 mmol) in toluene (2 mL) was added *N,N'*-1,3-bis(*P,P'*-di-isopropoxyphosphinic)-2,2-dimethylpropylenediamine (0.06 g, 0.15 mmol) in toluene (2 mL). The solution was stirred for 48 h before the solvents were removed *in vacuo* to leave a white solid, which was recrystallized from a minimum volume of hexane to give the product as colorless crystals (0.07 g, 72%).

¹H NMR (400 MHz, C₆D₆) δ ppm: 3.53 (dd, ³J_{HP} = 1.8 Hz, ²J_{HH} = 9.8 Hz, 1H, CH₂), 3.45 (dd, ³J_{HP} = 2.8 Hz, ²J_{HH} = 9.8 Hz, 1H, CH₂), 2.99 (dd, ³J_{HP} = 14.8 Hz, ²J_{HH} = 9.8 Hz, 1H, CH₂), 2.84 (dd, ³J_{HP} = 14.4 Hz, ²J_{HH} = 9.8 Hz, 1H, CH₂), 2.66 (spt, ³J_{HH} = 6.0 Hz, 1H, CH(CH₃)₂), 2.61 (spt, ³J_{HH} = 6.0 Hz, 1H, CH(CH₃)₂), 2.25 (spt, ³J_{HH} = 6.0 Hz, 1H, CH(CH₃)₂), 1.72 (spt, ³J_{HH} = 6.0 Hz, 1H, CH(CH₃)₂), 1.62 (dd, ³J_{HP} = 12.2 Hz, ³J_{HH} = 6.0 Hz, 3H, CHCH₃), 1.40 (dd, ³J_{HP} = 12.2 Hz, ³J_{HH} = 6.0 Hz, 3H, CHCH₃), 1.34 (dd, ³J_{HP} = 12.2 Hz, ³J_{HH} = 6.0 Hz, 3H, CHCH₃), 1.22 (dd,

³J_{HP} = 12.2 Hz, ³J_{HH} = 6.0 Hz, 3H, CHCH₃), 1.18 (s, 3H, CH₃), 1.15 (dd, ³J_{HP} = 12.2 Hz, ³J_{HH} = 6.0 Hz, 3H, CHCH₃), 1.11 (dd, ³J_{HP} = 12.2 Hz, ³J_{HH} = 6.0 Hz, 3H, CHCH₃), 1.08 (dd, ³J_{HP} = 12.2 Hz, ³J_{HH} = 6.0 Hz, 3H, CHCH₃), 0.80 (s, 3H, CH₃), 0.62 (s, 9H, Si(CH₃)₃), 0.53 (s, 9H, Si(CH₃)₃). ¹³C{¹H} NMR (100 MHz, C₆D₆) δ ppm: 55.7 (d, ²J_{CP} = 31.4 Hz, CH₂), 37.4 (s, C(CH₃)₂), 35.1 (d, ¹J_{CP} = 71.8 Hz, CH(CH₃)₂), 30.3 (d, ¹J_{CP} = 68.4 Hz, CH(CH₃)₂), 27.7 (s, CH₃), 27.5 (d, ¹J_{CP} = 60.5 Hz, CH(CH₃)₂), 25.4 (s, CH₃), 18.2 (35.1 (d, ²J_{CP} = 66.9 Hz, CHCH₃), 17.9 (35.1 (d, ²J_{CP} = 19.0 Hz, CHCH₃), 17.8 (d, ²J_{CP} = 45.0 Hz, CHCH₃), 17.2 (d, ²J_{CP} = 81.0 Hz, CHCH₃), 6.6 (s, Si(CH₃)₃), 6.3 (s, Si(CH₃)₃). ³¹P{¹H} NMR (162 MHz, C₆D₆) δ ppm: 65.4 (ddd, ²J_{PY} = 3.81, 3.08 Hz; ⁴J_{PP} = 1.86 Hz, 1P), 57.1 (dd, ²J_{PY} = 3.81 Hz; ⁴J_{PP} = 1.86 Hz, 1P). IR (Nujol mull, NaCl) ν cm⁻¹: 1263 (m, Si–CH₃ deformation), 1240 (m, P=O), 1223 (m, P=O), 1060 (m), 1014 (m), 999 (m). Anal. Calcd for C₁₈H₄₆N₃O₂P₂Si₂Y: 45.01, H, 9.20, N, 5.16. Found: 44.91, H, 9.15, N, 6.76.

4. To a solution of tris[*N,N'*-bis(di-isopropyl)amido]yttrium (0.13 g, 0.20 mmol) in toluene (0.5 mL) was added *N,N'*-1,3-bis(*P,P'*-di-isopropoxyphosphinic)-2,2-dimethylpropylenediamine (0.07 g, 0.20 mmol) in toluene (0.5 mL). The solution was stirred for 20 h before the solvents were removed *in vacuo* to leave a pale yellow solid, which was recrystallized from a minimum volume of hexane to give the product as pale yellow crystals (0.04 g, 71%).

¹H NMR (400 MHz, C₆D₆) δ ppm: 3.85 (spt, ³J_{HH} = 5.0 Hz, 1H, NCH(CH₃)₂), 3.34 (dd, ³J_{HP} = 3.2 Hz, ²J_{HH} = 8.4 Hz, 1H, CH₂), 3.32 (dd, ³J_{HP} = 3.2 Hz, ²J_{HH} = 8.4 Hz, 1H, CH₂), 3.08–2.90 (m, 3H, CH₂ and CH(CH₃)₂), 2.41 (d spt, ³J_{HH} = 6.0 Hz, ²J_{HP} = 14.4 Hz, 1H, CH(CH₃)₂), 1.79 (d spt, ³J_{HH} = 6.0 Hz, ²J_{HP} = 9.6 Hz, 1H, CH(CH₃)₂), 1.60 (d, ³J_{HH} = 5.0 Hz, 6H, NCH(CH₃)₂), 1.55 (dd, ³J_{HP} = 11.8 Hz, ³J_{HH} = 6.0 Hz, 3H, CHCH₃), 1.48 (d, ³J_{HH} = 5.0 Hz, 6H, NCH(CH₃)₂), 1.40 (dd, ³J_{HP} = 12.8 Hz, ³J_{HH} = 6.0 Hz, 3H, CHCH₃), 1.30–1.21 (m, 12H, CHCH₃ and CH₃), 1.12 (dd, ³J_{HP} = 12.0 Hz, ³J_{HH} = 6.0 Hz, 3H, CHCH₃), 1.09 (dd, ³J_{HP} = 11.2 Hz, ³J_{HH} = 6.0 Hz, 3H, CHCH₃), 1.08 (dd, ³J_{HP} = 11.2 Hz, ³J_{HH} = 6.0 Hz, 3H, CHCH₃), 0.88 (s, 3H, CH₃). ¹³C{¹H} NMR (100 MHz, C₆D₆) δ ppm: 57.6 (s, CH₂), 57.3 (s, CH₂), 37.6 (s, C(CH₃)₂), 31.9 (s, NCH(CH₃)₂), 31.8 (d, ²J_{CP} = 68.0 Hz, CH(CH₃)₂), 30.8 (d, ²J_{CP} = 68.9 Hz, CH(CH₃)₂), 28.8 (d, ²J_{CP} = 64.9 Hz, CH(CH₃)₂), 28.2 (s, NCH(CH₃)₂), 27.4 (s, NCH(CH₃)₂), 27.0 (d, ²J_{CP} = 66.9 Hz, CH(CH₃)₂), 26.3 (s, NCH(CH₃)₂), 24.9 (s, CH₃), 23.6 (s, CH₃), 18.7 (s, CH(CH₃)₂), 18.0 (s, CH(CH₃)₂), 17.5 (s, CH(CH₃)₂), 17.1 (s, CH(CH₃)₂), 17.0 (s, CH(CH₃)₂), 16.4 (s, CH(CH₃)₂). ³¹P{¹H} NMR (162 MHz, C₆D₆) δ ppm: 61.8 (ddd, ²J_{PY} = 5.45, 3.64 Hz; ⁴J_{PP} = 1.72 Hz, 1P), 57.1 (dd, ²J_{PY} = 4.55 Hz; ⁴J_{PP} = 1.72 Hz, 1P). IR (Nujol mull, NaCl) ν cm⁻¹: 2360 (w), 2341 (w), 1303 (m), 1225 (m, P=O), 1167 (m), 1068 (m), 1009 (m). Anal. Calcd for C₄₆H₁₀₄N₆O₄P₄Y₂: C, 49.91, H, 9.47, N, 7.59. Found: C, 50.08, H, 9.55, N, 7.51.

Lactide Polymerizations. All glassware was treated with Me₂–SiCl₂ (1 M solution in CH₂Cl₂) and oven-dried for 4 h prior to use. The lactide was dissolved in CH₂Cl₂ to make a 1 M solution. The initiator stock solution was in THF for **1** and in toluene for **2–4**. A portion of the initiator stock solution was added to a 1 M solution of *rac*-lactide in CH₂Cl₂ so that the lactide concentration was always 1 M. The polymerization was monitored by removal of aliquots at regular intervals. These were quenched by addition to wet hexane solutions, and the crude product was dried *in vacuo*. The percentage conversion was determined by integration of the signals in the ¹H NMR for the methine protons in polylactide (δ = 5.30–5.00 ppm) and lactide (δ = 4.92 ppm), respectively. The *M*_w, *M*_n, and PDI were determined by SEC in THF, calibrated using polystyrene and with a correction factor of 0.58 applied to the obtained *M*_n, as detailed in the literature.⁵⁵

Acknowledgment. The EPSRC is acknowledged for funding the research (grants EP/C544 846/1, EP/C544 838/1, GR/

T17960/01). Purac Plc. is thanked for the donation of *rac*-lactide. Mr. Peter Haycock is sincerely thanked for collecting and helping analyze the NMR spectroscopy.

Supporting Information Available: Numbering schemes and representations of the structures of **1** (Figure S1)¹⁹ and **2** (Figure

S2) and the X-ray crystallographic CIF file for **2**. Figure S3 shows the plot of $\ln\{[LA]_0/[LA]_t\}$ versus time for initiators **2** and **4**. This material is available free of charge via the Internet at <http://pubs.acs.org>.

OM7004194